International Transactions on Electrical Engineering and Computer Science
Kitmo et.al., Vol: 4, No: 3, pp: 137-151, September 2025

A Robust Maximum Power Point Tracking Control under Shading Effects on Photovoltaic Systems

Kitmo[1], Armel Duvalier Pene[2], Bikai Jacques[2], J. B. Bidias[2], Theodore Louossi[1], Doka Baza Gilbert[1], Kidmo Koaga Dieudonne[2], J. L. Nsouandele[1], Noël Djongyang[1], Cesar Kapseu[3]

Abstract: This article studies the behavior of a photovoltaic system under uncertain climatic conditions. The perturb and observe method is widely used in photovoltaic systems, but it encounters stability difficulties around maximum power points. The search for the maximum power point using the perturb and observe algorithms based on PSO is proposed using a PI controller. The proposed method enables the controller to follow the MPP perfectly, with less deviation from its trajectory. This method is applied to controlling the duty cycle of a boost converter. A test under variations in irradiance and temperature demonstrated the robustness of the method applied and its performance in terms of voltage and power stability. Simulation results obtained with MATLA/Simulink software show that MPPT-based PSO control can be used to improve the performance and efficiency of a photovoltaic system in domestic loads or industrial applications.

Keywords: Maximum Power Point Tracking, PV system, Partial shading, Power quality

1. Introduction

Nowadays, the optimization and efficiency of energy systems have become major issues for the development of any part of the planet [1]. This is why several methods are used. Among these methods, there are those that use empirical approaches and others that use advanced techniques such as algorithms.

History
Received: 10-04-2025; Revised: 18-06-2025;
Accepted: 20-08-2025

✉ Kitmo
kitmobahn@gmail.com
[1]University of Maroua, National Advanced School of Engineering of Maroua, Department of Renewable Energy, P.O. Box 58 Maroua, Cameroon.
[2]Department of Electrical Engineering, University Institute of Technology, University of Ngaoundere, Cameroon.
[3]Department of Process Engineering, National Advanced School of Agro-Industrial Industries, The University of Ngaoundere, Ngaoundéré, Cameroon.

https://doi.org/10.62760/iteecs.4.3.2025.144

Most of the advanced methods or techniques are based on human behavior or animal behavior. Other methods are also based on the behavior of plants or any other living species. The work in [2], heuristic methods based on PSO algorithms, is inspired by the behavior of bees in the evolution and search for solutions [3]. This is also the case in the work by [4], where a method based on the behavior of biological cells is employed. Several methods focus on the search for solutions using particles used as money in the search for solutions [5]. This is how algorithms are used because they integrate several particles or agents in the search for solutions in a specific space [6]; In the exploration space, we can generate as many particles and to multiply or expand the field of research of this investigation [7]. These techniques of algorithms based on particle swarms prove appropriate for the search for solutions in complex systems.

Although the P&O method appears to have a fast response time, it remains limited because it does not respond effectively to sudden changes in environmental conditions such as temperature or sunlight [8]. This method suffers from overshoots and oscillations. In this sense, it is necessary to find

methods that can adapt to varying environmental conditions without the risk of overshoot or oscillation, which is what allows us to demonstrate the robust performance of the algorithms. The Incremental Conductance (InC) method seems better suited to solve oscillation problems; but however, it is considered an old algorithm. Therefore, the P&O and InC algorithms are combined to capture the maximum power under partial shading conditions of photovoltaic systems [9].

Regarding the energy system based on renewable energies, where there is a variation in input parameters such as sunshine or temperature, the perturbed and observed method is much more commonly used by most scientific works. This justifies the fact that this method is based on perturbations or variations in time and space of the input variables of a continuous system. However, the P&O method is limited when there is a bus that changes the behavior of the system. This is how the work in [10], proposes the incremental method of conductance, while the work in [11], proposes the use of genetic algorithms. Besides these research works, we also have the work in [12], which proposes the use of BOA for the search for solutions in photovoltaic systems when it comes to improving performance [13]. The work in [14] shows that the use of TLBO in the photovoltaic system can improve yields, so a study is carried out on a solar system for powering the moves in a locality of Egypt was carried out using this method. An efficiency of 75% was evaluated using Teaching–Teaching-Learning-Based Optimization (TLBO) [15], however, the consideration of climatic parameters was not done on the one hand and on the other hand, the response time or the size of the particles was not highlighted. The work in [16] also specifies that genetic algorithms can be used for the search for solutions in complex systems. Similarly, in the work [17], the method of genetic algorithms is used to optimize the energy system of a hybrid PV wind system. In this work, the method used is also inspired by PSO algorithms to find solutions in an energy system consisting of photovoltaic generators [18].

Some algorithms are suitable for solving complex problems, but require a very long computation time, which makes them unusable in the management of energy systems that require fast computation or response time. In most algorithms used for optimizing energy systems, it is the duration of the response time that is important [19]. Some algorithms are used because they are simple to implement. Some calculation methods require data processing capacity while others require less storage space or information processing. The perturbed-observed method is much more commonly used because it is simple to implement. However, it uses direct data, which makes it limited when systems become complex. Photovoltaic systems are based on the generation of a current from a direct voltage source [20]. This is why the voltage and current are considered at the input of a photovoltaic generator. In order to effectively meet user specifications, it is advisable to use methods that limit the delay in processing information. This requirement results from the fact that there are several faults in electrical installations: for example, we have switching delay, very long response time, amplitude or frequency overshoot [21]. These are the hazards that make the energy system very energy-intensive. These defects reduce the efficiency of the installations. Among the most used methods in optimization systems, there is the TLBO, which is used in the work [16], for the optimization of a hybrid PV wind system. The same is true of genetic algorithms, which are used in the work in [22], for the improvement of the efficiency of the photovoltaic system. Regarding the work in [23], the modified PSO are used for the stability of distributed generation systems [24]. The photovoltaic system constitutes the main distributed generation, which is purely renewable in the same way as the wind system [25]. However, these systems also require recent and efficient methods. That is why we must use intelligent methods or those that integrate artificial intelligence. Among the variation parameters in the photovoltaic system, there are temperature, sunshine, and series resistance, which is also sometimes considered as variables. But in this work, we will focus on the effects of temperature variation and partial shading of solar cells. The study of partial shading is highlighted in this article. The same applies to the robustness of the PI controller [26], for controlling the duty cycle of the DC/DC converter [27]. The proposed method is a combination of the P&O algorithm with the PSO method. This approach will be compared to some used methods, such as the TLBO and GA algorithms [28].

2. Connected PV System and Partial Shading

The DC/DC converters are used for shaping DC signals in power generation. Some are used based on their performance in adapting to the sudden change in behavior of the input source, while others are used because they allow the highest possible voltage level to be raised [29]. Thus, the boost converter is the most widely used in the photovoltaic energy conversion system. This section is devoted to the study and modeling of the boost converter, which is used as an adaptation stage for the DC source from the photovoltaic generator. Fig. 1 depicts this illustration.

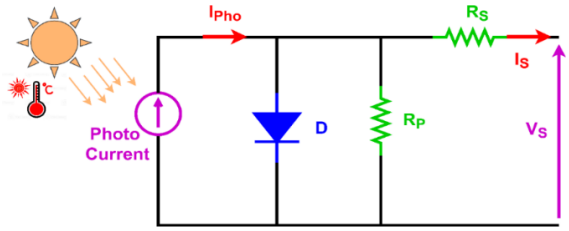

Fig. 1: Model of PV generator with one diode.

$$I = I_{PV} - I_D - I_{R_P} \tag{1}$$

$$I = I_{PV} - I_0\left[exp\left(\frac{V + R_s I}{a}\right) - 1\right] - \frac{V + R_s I}{R_P} \tag{2}$$

$$a = \frac{N_s nkT}{q} \tag{3}$$

The term I_0 represents the diode's reverse saturation or leakage current, which is a key parameter influencing the photovoltaic (PV) cell's performance [30-31]. The ideality factor, denoted as it, usually falls between 1 and 2 and offers insight into the recombination mechanisms within the diode. The symbol *Ns* indicates the total count of cells connected in series within the PV module, directly impacting the overall voltage produced. Additionally, the diode ideality constant *n* is a dimensionless value that helps describe the diode's behavior under varying conditions. The Boltzmann constant *k* (1.3806503 × 10−23−23 *J/K*) is a fundamental physical constant linking the average kinetic energy of gas particles with temperature, playing a crucial role in particle statistical mechanics [32]. The cell temperature *T*, measured in Kelvin, critically affects the thermal motion of charge carriers, which in turn influences the PV cell's current and voltage characteristics are presented in Equations (1) – (3). The electron charge q (1.60217646 × 10−19−19 C) is the fundamental electric charge of an electron and is essential for electrical calculations in semiconductor devices. Equation (4) details the current produced by the PV cell based on incident light while incorporating all these parameters [33]. This light-induced current is vital for converting solar energy into electrical power, as it directly converts the absorbed photons into a usable electric current. The relationships among these variables determine the PV cell's efficiency and effectiveness in solar energy harvesting [34]. Accurately understanding and calculating these factors is crucial for optimizing PV system design and ensuring maximum energy output and reliability [35].

$$I_{PV} = \left(I_{PV,n} + K_I\left(T - T_n\right)\right)\frac{G}{G_n} \tag{4}$$

The term $I_{PV,n}$ corresponds to the current produced by the photovoltaic (PV) cell under standard conditions, specifically at 25 °C and 1000 W/m² irradiance. The nominal temperature, T_n, expressed in Kelvin, is vital for analyzing the thermal characteristics of the PV cell [36]. The variable *G* stands for the actual solar irradiance received on the panel surface (in W/m²), which directly affects the electrical output, while G_n indicates the nominal irradiance value under standard test conditions. Equation (5) defines the diode's saturation current, I_0, which is a key parameter influencing the current-voltage behavior of the diode. This saturation current significantly impacts the PV cell's operational efficiency and performance across different environmental circumstances [37]. A thorough understanding of these factors is essential for accurately forecasting and optimizing the energy production of PV systems, thereby promoting efficient functionality under varying real-world conditions.

$$I_0 = \frac{I_{SC,n} + K_I\left(T - T_n\right)}{\exp\left(\frac{V_{OC,n} + K_V\left(T - T_n\right)}{a}\right) - 1} \tag{5}$$

The characteristics of the PV cells used in this work are given in the Table. 1 [38].

Table. 1: Characteristics of the PV cells

Parameters	Mono Crystalline
Model	SA-100
Maximum power (MP)	100 W
Maximum power voltage (MPV)	17.6 V
Maximum power current (MPC)	5.71 A
Open circuit voltage (OCV)	21 V
Short circuit current (SCC)	6.4 A
Number of cells (Ncells)	36
Dimensions (*D*)	1200 × 540 × 30 (mm)

The representation of the overall system is given in Fig. 2. This figure highlights the different components or stages of adaptation of photovoltaic energy. We have the photovoltaic source which is followed by a DC/DC converter. The DC converter is connected through a DC bus where the energy is taken, in order to be converted into alternating voltage for the load supply. The power is routed to the receiver via LC filtering [39].

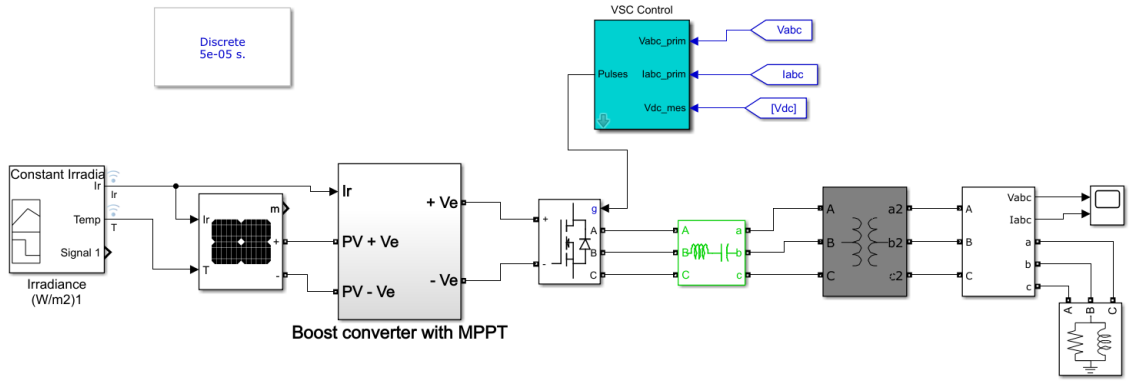

Fig. 2: Configuration of the system

3. Boost chopper energy control

A DC-to-DC converter has been implemented in this research, with its duty cycle actively managed by a Maximum Power Point Tracking (MPPT) system. The system utilizes a boost chopper [40], presented in Fig. 3, for energy conversion from the photovoltaic cells. The regulation of the chopper's duty cycle via the MPPT controller allows for the highest achievable power output. The characteristics of the chopper, shown in Fig. 3, are mathematically defined by Equations (6) and (7) [41]. These formulas provide the basis for the correct functioning of this power conversion stage, ensuring both maximum power extraction and simplified control of the duty cycle under optimal operating scenarios.

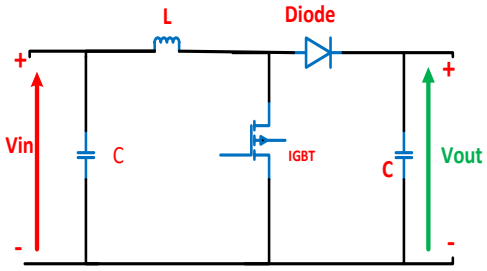

Fig. 3: Electrical circuit of the Boost converter

The selection of component values for the boost converter powered by a photovoltaic source was carried out according to standard engineering principles to ensure dependable operation, high efficiency, and a swift dynamic response even under varying conditions caused by partial shading. Specifically, the inductor and capacitor values were chosen based on these considerations: The inductance was sized to maintain continuous conduction mode throughout the full operating range, which reduces current ripple and improves overall efficiency. The minimum required inductance, denoted as L_{min}, was calculated using the formula below (6) [42].

$$L_{min} = \frac{V_{out} \times (V_{in} - V_{out})}{\Delta I_L \times f_s \, x V_{in}} \qquad (6)$$

In this context, V_{in} represents the voltage of the photovoltaic array, while V_{out} is the output voltage. The parameter ΔI_L refers to the target peak-to-peak ripple current in the inductor, typically set to about 25% of the average input current. The switching frequency is denoted by *fs* [43]. The output capacitor was selected to ensure that the voltage ripple remains within 1–2% of the output voltage V_{out}. The necessary capacitance value was determined using the following calculation (7).

$$C = \frac{I_{in} \times D}{\Delta V_{in} \times f_s} \quad (7)$$

where I_{in} is the output current, D is the duty cycle, and ΔV_{in} is the allowable voltage ripple. Based on these calculations and considering practical component availability and system dynamic requirements, the final component values were determined and used in the simulations.

4. Optimization of the power flow

The Maximum Power Point Tracking (MPPT) algorithm is a method used to optimize and capture the highest possible power from a given input signal. In this study, the approach implemented is a modified Perturb and Observe (P&O) model, with its process flow illustrated in Fig. 4 and Fig. 5. Fig. 3 presents a schematic of the MPPT chopper control system. The control system receives inputs such as the photocurrent generated and the voltage output from the solar panel. The DC is regulated to produce the desired chopper output voltage, which is supplied from the DC bus. The boost chopper is favored for its straightforward implementation, while the MPPT control helps increase the output voltage level efficiently. At the DC bus stage, energy can be conveniently stored in battery banks as a steady supply. DC loads can be powered directly from the DC bus, whereas AC loads require conversion through a DC-to-AC inverter. The configuration of boost converter input parameters is depicted in Fig. 4. This method uses direct photovoltaic array current and voltage data. The MPPT method, based on the perturb and observe method, is based on this approach.

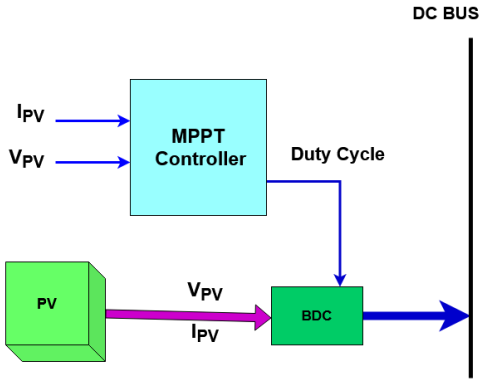

Fig. 4: Flowchart of MPPT algorithm using PV generator

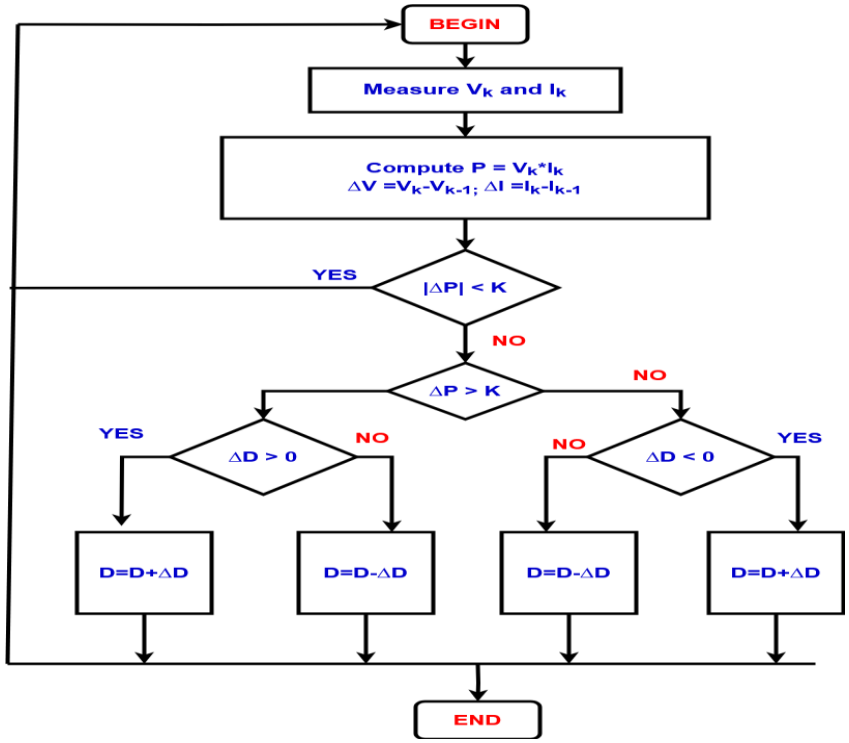

Fig. 5: Flowchart of the perturb and observe PV Algorithm

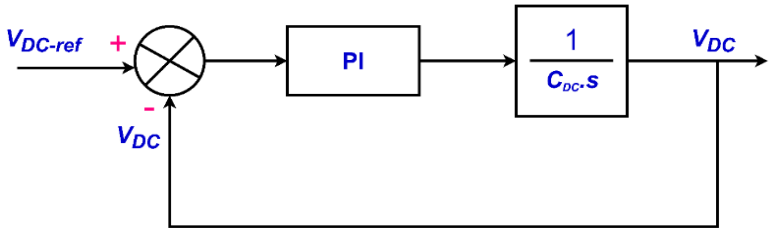

Fig. 6: Technique of duty cycle control

The method used is represented by the task flowchart shown in Fig. 5. This figure shows the various stages of duty cycle control you have dear voltage step-up. Thanks to the PI controller, the PSO-based P&O method stabilizes the output voltage of the DC converter after the power from the photovoltaic generator has been extracted. It is this voltage level that is injected via a DC bus, where an energy storage system can also be installed. As depicted in Fig. 5, the various steps of extracting the maximum power, the duty cycle is adjusted using the observed perturbation algorithms. The voltage level is adapted in the event of sudden variations of the input parameters in the solar system.

5. Adaptive Control of the DC/DC Converter

The proposed method uses the task flowchart, which presents the technique of evolving the sequences of tasks or generation processes and searching for optimal solutions. This technique is represented in Fig. 5. The different stages of the duty cycle control of the voltage boost chopper are also presented. Thanks to the PI controller, the Perturb and observe method, based on the PSO, allows stabilizing the output voltage of the DC converter after extracting the power from the photovoltaic generator. It is this voltage level that is injected through a continuous bus where an energy storage system that can also be installed. The boost converter is represented using Equation (8).

$$\begin{cases} L\dfrac{di_L}{dt} = V_d - Ri_L - (1-D)V_{DC} \\ C\dfrac{dV}{dt} = (1-D)i_L - \dfrac{V_{DC}}{R} - i_{DC} \end{cases} \quad (8)$$

The DC-AC converter can be modelled using Equation (9) [44].

$$i_{DC} = C_{DC}\frac{dV_{DC}}{dt} = i_L - i_{Conv} \quad (9)$$

The voltages at the output of the inverter are written as follows (10) [44]:

$$\begin{bmatrix} V_{\chi a} \\ V_{\chi b} \\ V_{\chi c} \end{bmatrix} = \frac{1}{3}V_{DC}\begin{bmatrix} 2 & -1 & -1 \\ -1 & 2 & -1 \\ -1 & -1 & 2 \end{bmatrix}\begin{bmatrix} \chi_1 \\ \chi_2 \\ \chi_3 \end{bmatrix} \quad (10)$$

Where χ_1, χ_2, and χ_3 are the switching function.

6. Strategy of voltage control

In renewable energy systems, regulating the bus voltage is vital for maximizing the efficiency of MPPT, as it directly impacts how effectively energy from sources like wind turbines or solar panels is delivered to the load. The closed-loop current of the DC-DC converter is obtained from Equation (11) [44], by applying the Laplace transform to derive the transfer function. This transfer function is then used to design the PI controller in the following form. The expression of the proportional integral control is given as,

$$F(s) = \frac{1}{(1+Ts)} \quad (11)$$

With $T = \dfrac{\xi}{V_{Dc}K_i}$

The proportional-integral (PI) controller [44]output is a combination of two terms: proportional control and integral control. It is mathematically expressed as,

$K_i = \dfrac{\xi}{T.V_{DC}}$ and $K_p = K_i\dfrac{L}{\xi}$

A standard PI controller needs to be placed before the converter to keep the DC bus voltage at the optimal level required by the load. In the Laplace domain, the closed-loop transfer function that includes this PI controller and the characteristic polynomial is expressed as follows (12) and (13) [45].

$$\frac{V_{DC}}{V_{DC-ref}} = \frac{\frac{K_p s + K_i}{C_{DC}}}{s^2 + \frac{K_p}{C_{DC}} s + \frac{K_i}{C_{DC}}} \quad (12)$$

$$P(s) = s^2 + \frac{K_p}{C_{DC}} s + \frac{K_i}{C_{DC}} \quad (13)$$

Where, *Ki* is the integral control and *Kp* is the proportional control. To find the expressions of the PI regulator, we impose two complex conjugate poles on the characteristic closed-loop polynomial (14): $S_{1,2} = \psi(1 \pm j)$ [46].

Where:

$$P(s) = s^2 + 2\psi^2 + 2\psi s \quad (14)$$

The identification of the two equations (15) and Equation (16) term by term allows us to write:

$$K_p = 2\psi C_{DC} \quad (15)$$

and

$$K_i = 2\psi^2 C_{DC} \quad (16)$$

7. Optimization of the photovoltaic system using the PSO strategy

Particle swarm optimization is formulated around particles that are defined according to their position X_i, their velocity V_i and their best position g_{best}. These particles are generated randomly in time and space, in order to locate the best position that corresponds to an ideal solution. These algorithms have operational and usage constraints. Most of the work on renewable energy uses PSO because it is faster compared to some algorithms such as the genetic algorithm or Whale Optimization Algorithm (WOA) [47]. Equation (17) represents the particle position, while equation (18) represents the particle velocity [47].

$$\begin{cases} V_i^{\alpha+1} = c_0 V_i^{\alpha} + c_1 r_{1i}^{\alpha}\left(X_i^{best,\alpha} - X_i^{\alpha}\right) \\ \quad + c_2 r_{2,i}^{\alpha}\left(X_{swarm}^{best,\alpha} - X_i^{\alpha}\right) \\ X_i^{\alpha+1} = X_i^{\alpha} + V_{i,j}^{\alpha+1} \end{cases} \quad (17)$$

$$\begin{cases} X_i^{best,\alpha} = \min\left\{\aleph\left(X_i^{j}\right), 0 \leqslant j \leqslant \alpha\right\} \\ X_{swarm}^{best,\alpha} = \min\left\{\aleph\left(X_i^{\alpha}\right), \forall i\right\} \end{cases} \quad (18)$$

8. Results and discussion

8.1 Effects of partial shading on the type of connection

The modeling results allow us to choose the type of solar cell combination. We can see that the series combination shown in Fig. 7 and extracts power better than the parallel combination shown in Fig. 8.

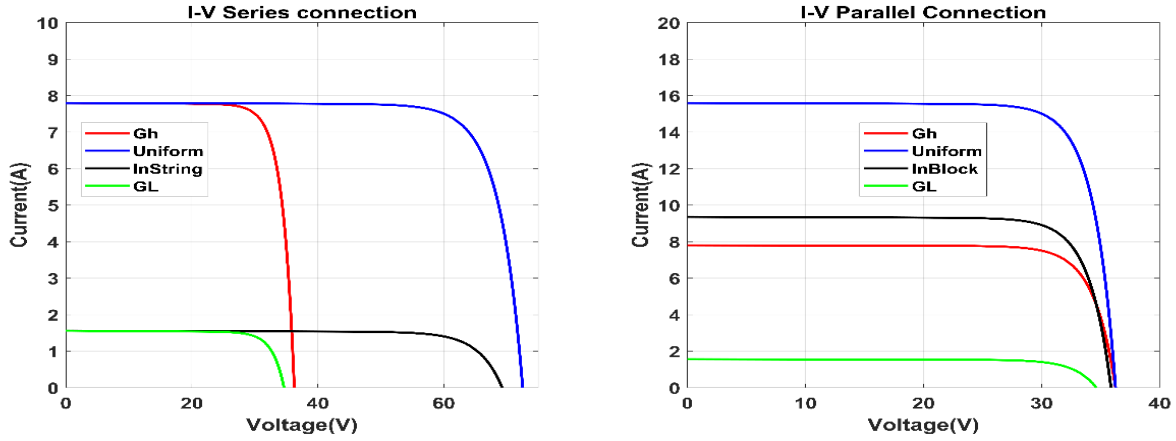

Fig. 7: Effects of the connection on the characteristics current/voltage

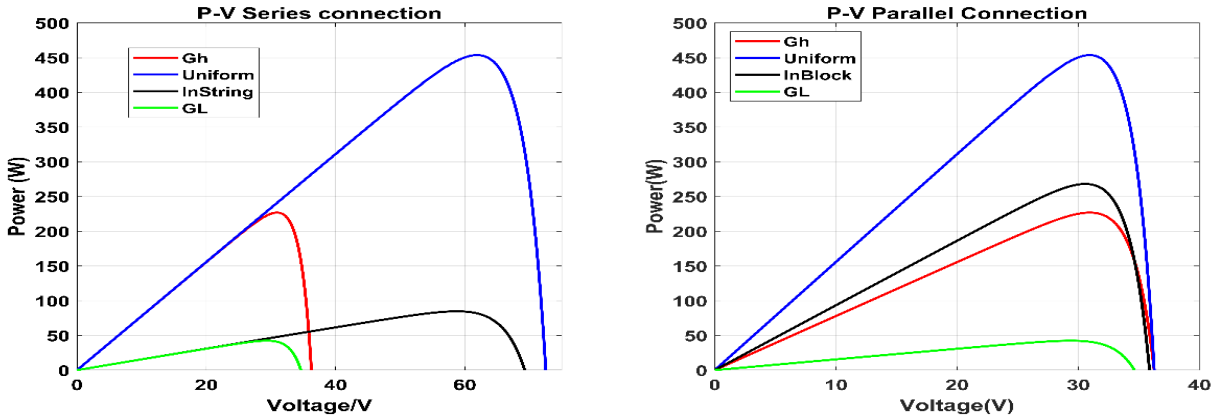

Fig. 8: Effects of shading on the characteristics power/voltage

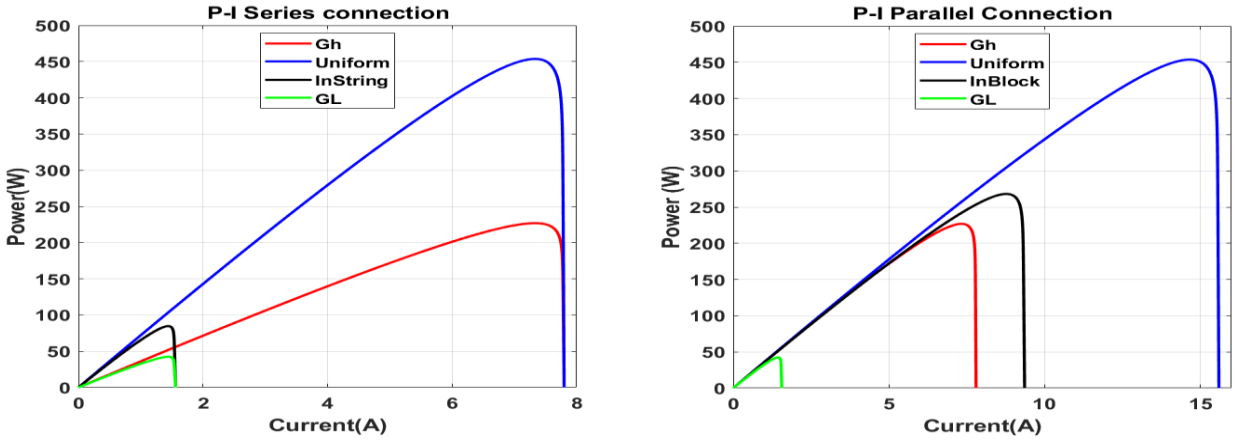

Fig. 9: Effects of the connection on the characteristics power/current

We observe a power of 45 kW for a voltage of 15 volts when the cells are connected in series, while a power of 12 volts is observed for a voltage of 15 W when the solar cells are connected in parallel. And these values have an influence on the quality of the energy produced, as depicted in Fig. 9.

8.2 Characteristics of the PV generator

The shading effects allow to obtain the characteristics of the photovoltaic generator for a sudden variation of the sunshine (GL) and for a gentle variation of the teaching (Gh), as depicted in Fig. 10. For the sudden variation we obtain a current of 7.9 A, while for a gentle shading we obtain a current of 1.5 A for a voltage of 30.4 V in the series connection scenario. For the parallel connection scenario, we obtain the current voltage values of 7.9 A, 38.2 V for the GL and 1.8 A, 37.5 V for the Gh. These characteristics show that the series association presents a robustness in case of sudden variation compared to the parallel association, but however does not deliver a better voltage compared to the parallel connection.

8.3 Effects of partial shading on the type of connection and on the power profile

In the same sense, an observation is made on the variation of the teaching in order to have an idea on the feasibility and the performance of the system as well as the proposed method. Thus, we observe in Fig. 10, the different variations of the irradiance which correspond to the power produced in the cases of partial shading scenarios of sudden or soft nature. We note that power peaks are observed for the variations of the teaching and the temperature but the PSO algorithm was able to stabilize the output voltage of the DC converter. The P&O method is not sufficient to produce such a performance because the conditions of

the evaluation are such that there is a sudden variation of the input elements of the converter. And it is shown that the P&O method is failing in the extraction of the maximum power when there is a sudden variation of the temperature or the sunshine [21]. It is then that the PSO algorithms are combined with the P&O method to have such a result. Also from Fig. 11 it is possible to clearly show that the proposed method exhibits robustness and reliability as well as feasibility in cases of little known weather conditions. The PV power and irradience are shown in Fig. 12.

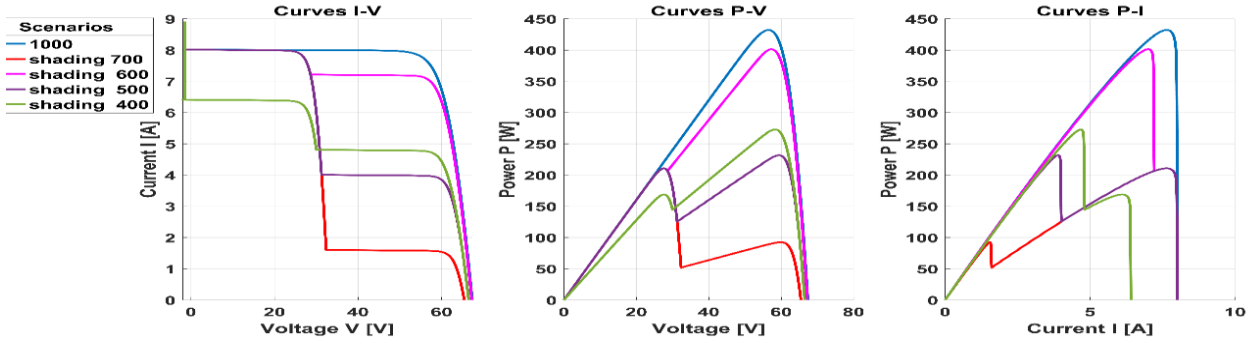

Fig. 10: characteristics power/current using four scenarios

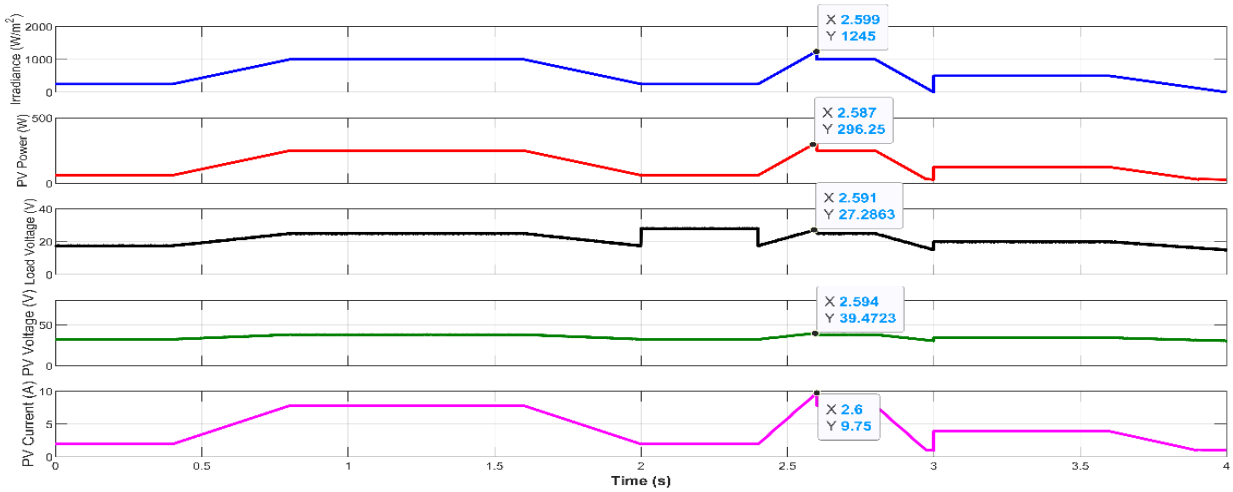

Fig. 11: Effects of the connection on the load voltage

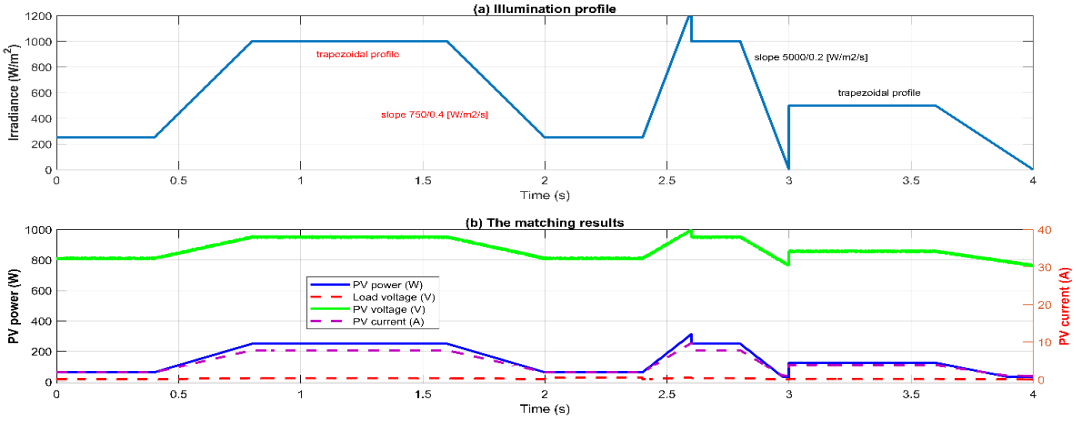

Fig.12: Effects of the connection on the PV voltage

8.4 Effects of partial shading on the maximum power points

The irradiances were varied and adjusted to see the behavior of the characteristics of the photovoltaic generator at the output of the continuous converter as depicted in Fig. 13. For the variations of 950W/m², 850W/m², 700W/m², 600 W/m², 700 W/m², 800 W/m², we obtain respectively the power values of 0.368kW, 0.3661 kW, 0.361 kW, 0.360 kW, 0.361 kW, 0.3611 kW, and 0.36 91 kW. The partial shading effects of 700 W/m² made it possible to deliver a current of 8 amps for a power of 448 watts, a current of 7 amps for a power of 400 watts, a current of 6.5 amps for a power of 250.5 watts, a current of 4 amps for a power of 240 watts and finally a current of 1.5 amps for a power of 60 watts. These values make it possible to stabilize the voltage around 30V for a scenario of a resistive load of 120.45Ω, under the evaluation conditions.

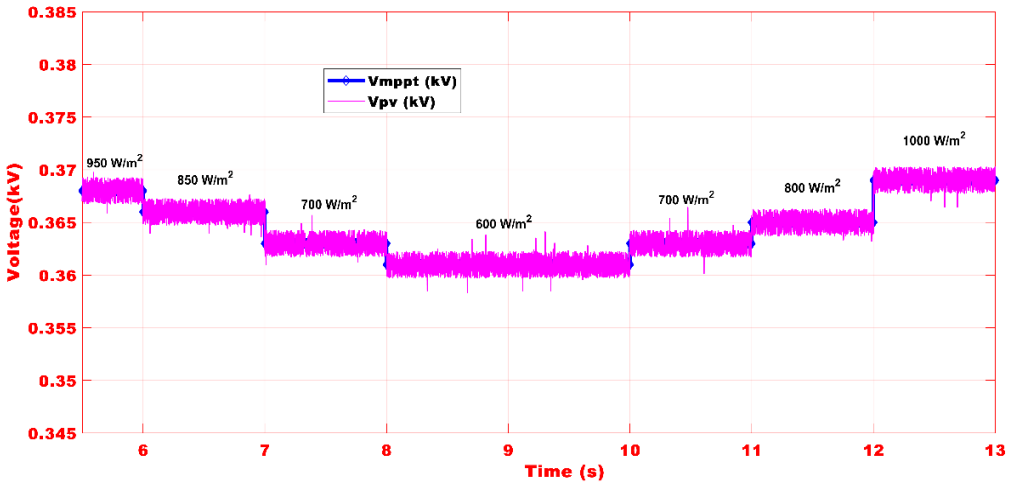

Fig. 13: Effects of the shading on the maximum voltage tracked

8.5 Performance of the PI controller

The disturbance effects are observed in Fig. 14. This figure shows that the genetic algorithms and the TLBO algorithms and method do not react quickly to reach saturation from the instant at t=3. Peaks are observed during this instant for these algorithms while the PSO algorithms follow a constant saturation. During the entire instant of evolution, we notice a slight improvement and increase for the PSO algorithms, which are largely above the algorithms whose values are respectively 341.02kW and 242.005 for the TLBO and the GA. At t equal to 3 seconds the TLBO and GA algorithms, produce respectively 157kW and 157.032kW. At t=0.3s, the TLBO produces a power of 247.7 and the GA provides 247.1 kW while the PSO algorithms produce a power of 248.03kW.

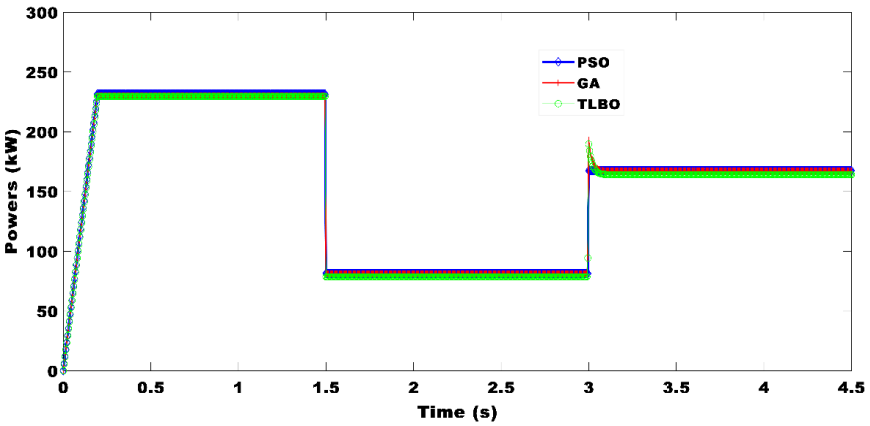

Fig. 14: Dynamic response of the system based PSO algorithms

Peaks are observed at t=3s. A voltage drop variation is observed in the interval from 1.5s to 3s. The maximum power is reached 1.5s up to 3s. These results show according to this approach the superiority of PSO algorithms over GA and TLBO, whatever the level of variation of sunlight or temperature. The power profiles are presented in Fig.15. The robustness of each algorithm is shown by the ability to extract more power and stabilize the power level. It is observed that the proposed PSO improves the power level better compared to genetic algorithms which in turn is better compared to the TLBO method. The variation in the capacities of each generated power is a consequence of disturbance of the sunshine or the temperature at the solar cells. For variations in sunshine or in the presence of partial shading, genetic algorithms and TLBO algorithms are less robust compared to PSO algorithms. PSO algorithms have the ability to converge quickly to the solutions. We obtain a value of 90 kW for the PSO and 57 kW for the GA and a value of 47 kW for the TLBO. Furthermore, it is noted that the PSO algorithms are robust to transient disturbances. During the time instants ranging from 0 to 4s to 6 and from 0 to 7s, we observe strong disturbances. These fluctuations in power cause enormous power losses. This justifies the fact that when the delay is very large, voltage drops sometimes lead to blackouts if the distributed generation systems do not operate in islanding. Moreover, when the response time is fast, power losses are limited and the stability of the system is also improved.

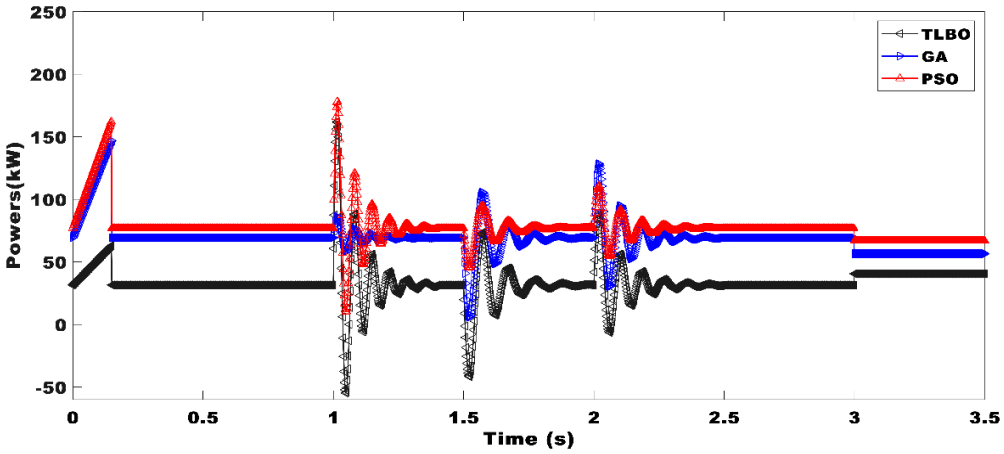

Fig. 15: Performances of the PSO algorithms

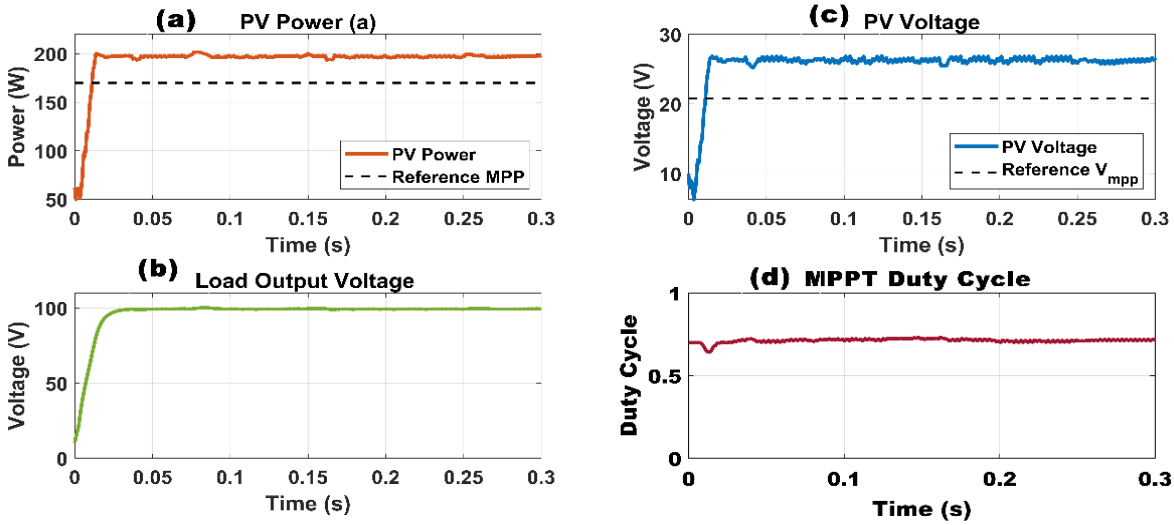

Fig. 16: Stabilization of the DC/DC converter

8.6 Effects of partial shading on the DC/DC converter

The regulation of the voltage level by controlling the duty cycle of the boost converter made it possible to have the power voltage profile as well as the operating interval of the duty cycle. A voltage of 100 volts is supplied to the load for a duty cycle that varies from 0.54 to 0.55. A power is delivered at 200 watts, which corresponds to a maximum power extracted at 28 volts for a reference that is constant of 21 volts. The voltage level regulation as well as the stabilization of the voltage level and obtained. The regulated and stabilized voltage is well above the reference. This Fig. 16 is obtained thanks to the combination of PSO algorithms based on the perturbed-observed method, which consists of searching for the maximum power for variations of the input parameters. The advantage of the MPPT perturb and observe control lies in the fact that it quickly approaches the reference power, while the particularity of the PSO algorithms lies in the fact that they are fast and allow for convergence towards the solutions as quickly as possible compared to algorithms such as the genetic algorithm or the TLBO method. The stabilization and the voltage level regulation obtained in Fig. 16 allow to demonstrate the robustness of the proposed method as well as its reliability in extracting the maximum power from a photovoltaic generator.

9. Conclusion

The study of meteorological data such as temperature and solar irradiance has enabled us to assess the robustness of the P&O PSO algorithms. Solar cell shading effects demonstrate the stability and performance of the proposed approach to photovoltaic system optimization. After varying temperature and sunshine, the proposed method showed superiority over certain algorithms such as TLBO or the genetic algorithm. This method is also compared with the traditional approach, which is based on the use of direct data from the input parameters of a photovoltaic system. The system's ability to respond to sudden oscillations and reduce power overshoots demonstrates the reliability and robustness of the method used. A study of the algorithm's performance shows that the P&O based-PSO method is better at extracting power from a photovoltaic array.

References

[1] K. D. Goron, B. Jacques, C. Babé, and N. Djongyang, "Improvement of photovoltaic power plant energy and harmonic attenuation for grid enhancement", *International Journal of Energy Power Engineering*, Vol. 14, No. 2, pp. 50–62, 2025. https://doi.org/10.11648/j.ijepe.20251402.13

[2] S. Liu *et al.*, "Integration method of large-scale photovoltaic system in distribution network based on improved multi-objective TLBO algorithm", *Frontiers in Energy Research*, Vol. 11, art. no. 1322111, 2023. https://doi.org/10.3389/fenrg.2023.1322111

[3] Kitmo, G. B. Tchaya, and N. Djongyang, "Optimization of hybrid grid-tie wind solar power system for large-scale energy supply in Cameroon", *International Journal of Environmental Engineering*, Vol. 14, No. 4, pp. 777–789, 2023. https://doi.org/10.1007/s40095-022-00548-8

[4] A. Gautam, Ibraheem, G. Sharma, M. Kumawat, and M. F. Ahmer, "A novel solution for the power transmission congestion of deregulated power system using TCSC and TLBO algorithm", *Electrical Engineering and Electronics Energy*, Vol. 8, art. no. 100592, 2024. https://doi.org/10.1016/j.prime.2024.100592

[5] S. Acharya, S. Das, and X. Kitmo, "Adaptive learning and self-organization in swarm robotics", *Bio-inspired Swarm Robotics and Control: Algorithms, Mechanisms, and Strategies*, pp. 116–139, 2024. http://dx.doi.org/10.4018/979-8-3693-1277-3.ch008

[6] S. Alphonse *et al.*, "Optimization PV/Batteries system: application in wouro kessoum village ngaoundere cameroon", *Journal of Power Energy Engineering*, Vol. 9, No. 11, pp. 50–59, 2021. http://dx.doi.org/10.4236/jpee.2021.911003

[7] G. Byanpambé *et al.*, "A modified fractional short circuit current MPPT and multicellular converter for improving power quality and efficiency in PV chain", *PLoS One*, Vol. 19, No. 9, art. no. e0309460, 2024. https://doi.org/10.1371/journal.pone.0309460

[8] B. Bogno *et al.*, "Enhancing the power quality in radial electrical systems using optimal sizing and selective allocation of distributed generations", *PLoS One*, Vol. 19, No. 12, art. no. 0316281, 2024. https://doi.org/10.1371/journal.pone.0316281

[9] M. F. Elnaggar *et al.*, "Optimal sizing and power losses reduction of photovoltaic systems using PSO and LCL filters", *PLoS One*, Vol. 19, No. 4, art. no. e0301516, 2024. https://doi.org/10.1371/journal.pone.0301516b

[10] A. Taïssala, N. Djongyang, A. Tom, and N. Nicodem, "A modified perturb and observe maximum power point tracking algorithm for a standalone single phase photovoltaic system using boost converter", *Journal of Renewable Energies*, Vol. 21, pp. 575–591, 2018. https://doi.org/10.54966/jreen.v21i4.713

[11] H. De Battista, P. F. Puleston, R. J. Mantz, and C. F. Christiansen, "Sliding mode control of wind energy systems with DOIG-power efficiency and torsional dynamics optimization", *IEEE Transactions On Power Systems*, Vol. 15, No. 2, pp. 728–734, 2000. https://doi.org/10.1109/59.867166

[12] J. S. Koh, R. H. G. Tan, W. H. Lim, and N. M. L. Tan, "A modified particle swarm optimization for efficient maximum power point tracking under partial shading condition", *IEEE Transactions on Sustainable Energy*, Vol. 14, No. 3, pp. 1822-1834, 2023. https://doi.org/10.1109/TSTE.2023.3250710

[13] S. K. Sahu, K. Mazumdar, B. Kitmo, Y. B. Jember, and S. Das, "Design and investigation of InGaAs/InP/InAlAs MOSFET with optimized switching efficiency", *IEEE Access*, Vol. 12, pp. 70045 - 70052, 2024. https://doi.org/10.1109/ACCESS.2024.3401851

[14] R. B. Singh, R. P. Payasi, and K. S. Verma, "Optimal allocation of distributed generation in order to improve the performance of power system networks", *ICT Analysis and Applications*, Vol. 314, pp. 677–690, 2022. https://doi.org/10.1007/978-981-16-5655-2_65

[15] A. Boussaibo, A. D. Pene, K. , A. Boussaibo, A. D. Pene, and K. , "Optimal sizing and power losses reduction of photovoltaic systems using pvsyst software", *Journal of Power Energy Engineering*, Vol. 12, No. 7, pp. 23–38, 2024. https://doi.org/10.4236/jpee.2024.127002

[16] Kitmo, G. B. Tchaya, and N. Djongyang, "Optimization of the photovoltaic systems on the North Cameroon interconnected electrical grid", *International Journal of Energy and Environmental Engineering*, Vol. 13, No. 1, pp. 305–317, 2021. https://doi.org/10.1007/s40095-021-00427-8

[17] P. Kumar, S. N. Singh, and S. Dawra, "Software component reusability prediction using extra tree classifier and enhanced Harris hawks optimization algorithm", *International Journal System Assurance Engineering and Management*, Vol. 13, No. 2, pp. 892–903, 2022. https://doi.org/10.1007/s13198-021-01359-6

[18] J. Divya Navamani, K. Boopathi, M. Jagabar Sathik, A. Lavanya, Kitmo, and P. Vishnuram, "Analysis of higher dimensional converter using graphical approach", *IEEE Access*, Vol. 11, pp. 75076-75092, 2023. https://doi.org/10.1109/ACCESS.2023.3295996

[19] Kitmo, G. B. Tchaya, and N. Djongyang, "Optimization of the photovoltaic systems on the north cameroon interconnected electrical grid", *International Journal of Energy Environmental and Engineering*, Vol. 13, No. 1, pp. 305–317, 2022. https://doi.org/10.1007/s40095-021-00427-8

[20] B.-P. Ngoussandou *et al.*, "Optimal energy scheduling method for the north cameroonian interconnected grid in response to load shedding", *Sustainable Energy Research*, Vol. 14, art. no. 14, 2023. https://doi.org/10.1186/s40807-023-00084-x

[21] K. Null, C. Babé, N. Nicodem, K. Bernard, and N. Djongyang, "Selective allocation of distributed photovoltaic systems using experimental data from tropical areas", *International Journal Sustainable Green Energy*, Vol. 14, No. 3, pp. 160–170, 2025. https://doi.org/10.11648/j.ijsge.20251403.13

[22] Y. Akarne, A. Essadki, T. Nasser, H. Laghridat, and B. El Bhiri, "Enhanced power optimization of photovoltaic system in a grid connected AC microgrid under variable atmospheric conditions using PSO-MPPT technique",2023 *4th International Conference Clean Green Energy Engineering (CGEE)*, pp. 19–24, 2023. https://doi.org/10.1109/CGEE59468.2023.10351965

[23] S. Usha, T. M. ThamizhThentral, R. Palanisamy, A. Geetha, P. Geetha, and Kitmo, "Mitigation of circulating current and common mode voltage in grid-connected induction motor drive using modified PID-fuzzy controller", *Multiscale Multidisciplinary Modelling, Experiments and*

Design, Vol.7, pp. 233-247, 2023. https://doi.org/10.1007/s41939-023-00192-7

[24] A. F. Minai *et al.*, "Evolution and role of virtual power plants: Market strategy with integration of renewable based microgrids", *Energy Strategy Reviews*, Vol. 53, art. no. 101390, 2025. https://doi.org/10.1016/j.esr.2024.101390

[25] K. K. Dieudonne, M. Bajaj, Kitmo, O. Rubanenko, F. Jurado, and S. Kamel, "Hydropower potential assessment of four selected sites in the north interconnected network of cameroon", *2022 IEEE International Conference on Automation/XXV Congress of the Chilean Association of Automatic Control (ICA-ACCA)*, pp. 1-6, 2022. https://doi.org/10.1109/ICA-ACCA56767.2022.10005948

[26] S. Usha, T. M. ThamizhThentral, R. Palanisamy, A. Geetha, P. Geetha, and Kitmo, "Mitigation of circulating current and common mode voltage in grid-connected induction motor drive using modified PID-fuzzy controller", *Multiscale Multidisciplinary Modelling, Experiments and Design*, Vol. 7, pp. 233-247, 2023. https://doi.org/10.1007/s41939-023-00192-7

[27] B.-P. Ngoussandou, N. Nisso, D. K. Kidmo, and Kitmo, "Optimal placement and sizing of distributed generations for power losses minimization using PSO-based deep learning techniques", *Smart Grid Renewable Energy*, Vol. 14, No. 9, pp. 169–181, 2023. https://doi.org/10.4236/sgre.2023.149010

[28] T. E. K. Zidane *et al.*, "Grid-connected solar PV power plants optimization: A review", *IEEE Access*, Vol. 11, pp. 79588-79608, 2023. https://doi.org/10.1109/ACCESS.2023.3299815

[29] Yaouba *et al.*, "An experimental and case study on the evaluation of the partial shading impact on pv module performance operating under the sudano-sahelian climate of cameroon", *Frontiers in Energy Research*, Vol. 10, art. no. 924285, 2022. https://doi.org/10.3389/fenrg.2022.924285

[30] C. Meira Amaral da Luz, E. Roberto Ribeiro, and F. Lessa Tofoli, "Analysis of the PV-to-PV architecture with a bidirectional Buck-Boost converter under shading conditions", *Solar Energy*, Vol. 232, pp. 102–119, 2022. https://doi.org/10.1016/j.solener.2021.12.028

[31] N. Bello-Pierre *et al.*, "Energy efficiency in periods of load shedding and detrimental effects of energy dependence in the city of maroua, cameroon", *Smart Grid Renewable Energy*, Vol. 14, No. 4, pp. 61–71, 2023. https://doi.org/10.4236/sgre.2023.144004

[32] R. Palanisamy, M. Singh, R. Ramkumar, S. Usha, T. M. T. Thentral, and Kitmo, "Capacitor voltage unbalance minimization for three-phase five-level diode clamped inverter using hexagonal hysteresis space vector modulation," *Multiscale Multidisciplinary Modelling, Experiments and Design*, pp. 1–11, 2023. https://doi.org/10.4236/sgre.2023.144004

[33] E. M. Molla and C. C. Kuo, "Voltage sag enhancement of grid connected hybrid PV-wind power system using battery and SMES based dynamic voltage restorer", *IEEE Access*, Vol. 8, pp. 130003 – 130013, 2020. https://doi.org/10.1109/ACCESS.2020.3009420

[34] R. Djidimbélé, B. P. Ngoussandou, D. K. Kidmo, Kitmo, M. Bajaj, and D. Raidandi, "Optimal sizing of hybrid systems for power loss reduction and voltage improvement using PSO algorithm: Case study of guissia rural grid", *Energy Reports*, Vol. 8, pp. 86–95, 2022. https://doi.org/10.1016/j.egyr.2022.06.093

[35] C. Saiprakash, A. Mohapatra, B. Nayak, and S. R. Ghatak, "Analysis of partial shading effect on energy output of different solar PV array configurations", *Materials Today Procedings*, Vol. 39, pp. 1905–1909, 2021. https://doi.org/10.1016/j.matpr.2020.08.307

[36] M. Haris *et al.*, "Genetic algorithm optimization of heliostat field layout for the design of a central receiver solar thermal power plant", *Heliyon*, Vol. 9, No. 11, 2023. https://doi.org/10.1016/j.heliyon.2023.e21488

[37] S. Sakar, M. E. Balci, S. H. E. Abdel Aleem, and A. F. Zobaa, "Increasing PV hosting capacity in distorted distribution systems using passive harmonic filtering", *Electrical Power System Research*, Vol. 148, pp. 74–86, 2017. https://doi.org/10.1016/j.epsr.2017.03.020

[38] A. Boussaibo *et al.*, "Impact of laterite and silt dust deposition on crystalline panels under local weather conditions: case of the northern zone of cameroon", *Energy and Power Engineering*, Vol. 17, No. 7, pp. 155–168, 2025.

http://dx.doi.org/10.4236/epe.2025.177008

[39] Kitmo and M. M. Rahman, "Investments in energy complexes: evidence from tajikistan", *Decision Making in Interdisciplinary Renewable Energy Projects*, pp. 209–219, 2024. https://doi.org/10.1007/978-3-031-51532-3_17

[40] Kitmo, R. Djidimbélé, D. K. Kidmo, G. B. Tchaya, and N. Djongyang, "Optimization of the power flow of photovoltaic generators in electrical networks by MPPT algorithm and parallel active filters", *Energy Reports*, Vol. 7, pp. 491–505, 2021. https://doi.org/10.1016/j.egyr.2021.07.103

[41] W. Chaichan, J. Waewsak, R. Nikhom, C. Kongruang, S. Chiwamongkhonkarn, and Y. Gagnon, "Optimization of stand-alone and grid-connected hybrid solar/wind/fuel cell power generation for green islands: application to Koh Samui, southern thailand", *Energy Reports*, Vol. 8, pp. 480-493, 2022. https://doi.org/10.1016/j.egyr.2022.07.024

[42] S. Lu, N. B. Schroeder, H. M. Kim, and U. V. Shanbhag, "Hybrid power/energy generation through multidisciplinary and multilevel design optimization with complementarity constraints", *Journal of Mechanical Design*, Vol. 132, No. 10, art. no. 101007, 2010. https://doi.org/10.1115/1.4002292

[43] M. R. Abdussami, M. I. Adham, and H. A. Gabbar, "Modeling and performance analysis of nuclear renewable micro hybrid energy system based on different coupling methods", *Energy Reports*, Vol. 6, pp. 189–206, 2020. https://doi.org/10.1016/j.egyr.2020.08.043

[44] L. R. Visser, E. M. B. Schuurmans, T. A. AlSkaif, H. A. Fidder, A. M. V. Voorden, and W. G. J. H. M. V. Sark, "Regulation strategies for mitigating voltage fluctuations induced by photovoltaic solar systems in an urban low voltage grid", *International Journal of Electronics Power Energy System*, Vol. 137, 2022. https://doi.org/10.1016/j.ijepes.2021.107695

[45] Z. Wang *et al.*, "Study on the optimal configuration of a wind solar battery fuel cell system based on a regional power supply", *IEEE Access*, Vol. 9, pp. 47056 - 47068, 2021. https://doi.org/10.1109/ACCESS.2021.3064888

[46] P. D. Necoechea-Porras, A. López, and J. C. Salazar Elena, "Deregulation in the energy sector and its economic effects on the power sector: A literature review", *Sustainability*, Vol. 13, No. 6, art. no. 3429, 2021. https://doi.org/10.3390/su13063429

[47] M. J. B. Kabeyi and O. A. Olanrewaju, "Sustainable energy transition for renewable and low carbon grid electricity generation and supply", *Frontiers in Energy Research*, Vol. 9, art. no. 743114, 2022. https://doi.org/10.3389/fenrg.2021.743114

***